Ultrasound-induced lung hemorrhage: Role of acoustic boundary conditions at the pleural surface

William D. O'Brien, Jr.
Bioacoustics Research Laboratory, Department of Electrical and Computer Engineering, University of Illinois, 405 North Mathews, Urbana, Illinois 61801

Jeffrey M. Kramer and Tony G. Waldrop
Department of Molecular and Integrative Physiology, University of Illinois, 407 South Goodwin, Urbana, Illinois 61801

Leon A. Frizzell and Rita J. Miller
Bioacoustics Research Laboratory, Department of Electrical and Computer Engineering, University of Illinois, 405 North Mathews, Urbana, Illinois 61801

James P. Blue and James F. Zachary
Department of Veterinary Pathobiology, University of Illinois, 2001 South Lincoln Avenue, Urbana, Illinois 61802

(Received 10 July 2001; accepted for publication 21 November 2001)

In a previous study [J. Acoust. Soc. Am. **108**, 1290 (2000)] the acoustic impedance difference between intercostal tissue and lung was evaluated as a possible explanation for the enhanced lung damage with increased hydrostatic pressure, but the hydrostatic-pressure-dependent impedance difference alone could not explain the enhanced occurrence of hemorrhage. In that study, it was hypothesized that the animal's breathing pattern might be altered as a function of hydrostatic pressure, which in turn might affect the volume of air inspired and expired. The acoustic impedance difference between intercostal tissue and lung would be affected with altered lung inflation, thus altering the acoustic boundary conditions. In this study, 12 rats were exposed to 3 volumes of lung inflation (*inflated*: approximately tidal volume; *half-deflated*: half-tidal volume; *deflated*: lung volume at functional residual capacity), 6 rats at 8.6-MPa *in situ* peak rarefactional pressure (MI of 3.1) and 6 rats at 16-MPa *in situ* peak rarefactional pressure (MI of 5.8). Respiration was chemically inhibited and a ventilator was used to control lung volume and respiratory frequency. Superthreshold ultrasound exposures of the lungs were used (3.1-MHz, 1000-Hz PRF, 1.3-μs pulse duration, 10-s exposure duration) to produce lesions. Deflated lungs were more easily damaged than half-deflated lungs, and half-deflated lungs were more easily damaged than inflated lungs. In fact, there were no lesions observed in inflated lungs in any of the rats. The acoustic impedance difference between intercostal tissue and lung is much less for the deflated lung condition, suggesting that the extent of lung damage is related to the amount of acoustic energy that is propagated across the pleural surface boundary. [DOI: 10.1121/1.1436068]

PACS numbers: 43.80.Cs, 43.80.Gx, 43.80.Jz [FD]

I. INTRODUCTION

A considerable amount of work has been published regarding lung hemorrhage caused by ultrasound.[1–21] There is agreement that gas in the lung plays a role in the ultrasound-induced damage mechanism, and that the mechanism is nonthermal. A distinction needs to be made between mechanisms involving large gas bodies, such as gas in the alveoli of the lung (38–49 μm),[22–24] and classical inertial cavitation that involves small microbubbles as nuclei (radii on the order of 1 μm or less).[25] Evidence has been slowly accumulating that suggests that the mechanism of damage in the lung may not be inertial cavitation. There seems to be no dependence on whether the positive or negative components of the ultrasonic pulse cause lithotripter-induced lung damage; however, inertial cavitation is associated with negative pressure.[26] The frequency dependence may not be the same as that associated with effects due to the presence of contrast agents that quite clearly nucleate inertial cavitation.[27] The hydrostatic pressure dependence of ultrasound-induced lung hemorrhage in mice is not the same as that associated with effects due to inertial cavitation.[17] Likewise, there is evidence that suggests the mechanism of damage in rat lung may be inertial cavitation.[9,28] However, the goal of this contribution is not to strengthen or weaken the arguments for or against inertial cavitation; the debate will probably continue for some time.[29–32] The goal is to inform the community of an interesting nonthermal observation that affects the degree of ultrasound-induced lung damage.

The study reported herein was motivated by an interesting finding that showed that the amount of lung damage was greater under increased hydrostatic pressure.[17] The acoustic impedance difference between intercostal tissue and lung was evaluated as a possible explanation for the enhanced lung damage with increased hydrostatic pressure, but hydrostatic-pressure-dependent impedance difference along could not explain the enhanced effects on hemorrhage. In

that study, it was hypothesized that the mouse's breathing pattern might be altered as a function of hydrostatic pressure, which in turn, might affect the volume of air inspired and expired by the mouse. With altered lung inflation, the acoustic impedance difference between intercostal tissue and lung would be affected thus affecting the acoustic boundary conditions. This brief report describes an experiment and some simple acoustic theory to provide insight into the mechanism of ultrasound-induced lung hemorrhage under *in vivo* conditions in which rats were subjected to three levels of lung inflation during ultrasound exposure.

II. ANIMAL EXPERIMENTS

A. Exposimetry

The exposimetry and calibration procedures have been described previously in detail[17,18] Ultrasonic exposures were conducted using one focused, 51-mm-diameter, lithium niobate ultrasonic transducer (Valpey Fisher, Hopkinton, MA). Water-based (distilled water, 22 °C) pulse-echo ultrasonic field distribution measurements were performed according to established procedures[33] and yielded a center frequency of 3.1 MHz, a fractional bandwidth of 15%, a focal length of 56 mm, a −6-dB focal beamwidth of 610 μm, and a −6-dB depth of focus of 5.9 mm.

An automated procedure described previously was used routinely to calibrate the ultrasound field.[17,18,34–36] The source transducer was mounted in a water tank (degassed water, 22 °C) and its drive voltage was supplied by a RAM5000 (Ritec, Inc., Warwich, RI). Calibrations were performed with a PVDF calibrated hydrophone (Marconi Model Y-34-6543, Chelmsford, UK). The *in situ* (at the pleural surface) pressure values were estimated using linear theory from procedures previously described.[18] They were estimated from measured *in vitro* peak rarefactional pressure of 10.1 and 18.9 MPa (s.d.'s=0.5 and 1.2 MPa, n=13), measured *in vitro* peak compressional pressure of 21.9 and 46.5 MPa (s.d.'s=1.9 and 1.6 MPa, n=13), an intercostal tissue attenuation coefficient of 1.1 dB/cm MHz,[37] and a mean chest wall thickness of 4.05 mm (s.d.=0.09 mm, n=12). The two *in situ* peak rarefactional pressures, $p_{r(in\ situ)}$, were 8.6 and 16 MPa and the respective *in situ* peak compressional pressures, $p_{c(in\ situ)}$, were 18 and 40 MPa. For comparison to a quantity that appears on the display of diagnostic ultrasound equipment,[35] the Mechanical Indices were 3.1 and 5.6, and were determined according to the procedures specified by the standard.[18,35] These exposure levels were known to be superthreshold values based on previous studies[18–20] where ultrasound exposures were conducted on normal-breathing animals.

B. Animals

The experimental protocol was approved by the campus Laboratory Animal Care Advisory Committee and satisfied all University of Illinois and NIH rules for the humane use of laboratory animals. Animals were housed in an AAALAC-approved animal facility, placed in groups of three or four in polycarbonate cages with beta-chip bedding and wire bar lids, and provided food and water *ad libitum*.

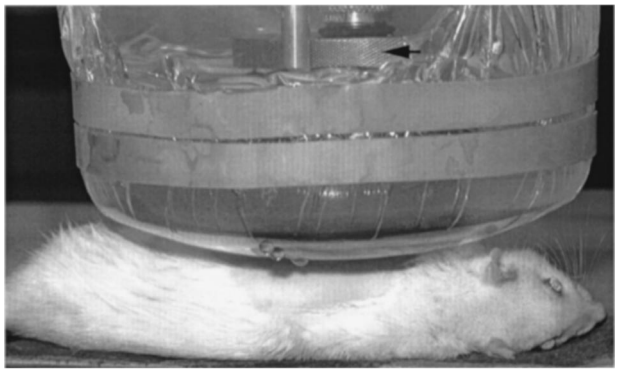

FIG. 1. Photograph showing the rat in right lateral recumbancy with the water-filled stand-off tank positioned in contact with the skin. The arrow points to the 3.1-MHz transducer.

Twelve 230-g (s.d.=10 g) 10-to-11 week-old Sprague-Dawley rats (Harlan, Indianapolis, IN) were initially anesthetized with an intraperitoneal injection of Ketamine (87 mg/kg) and Rompun (13 mg/kg). The rats were randomly assigned to one of three ultrasound exposure groups: sham (2 rats), $p_{r(in\ situ)}$=8.6 MPa (6 rats) and $p_{r(in\ situ)}$=16 MPa (6 rats). Additional doses of anesthetic were administered upon evidence of foot withdrawal to noxious paw pinch. The individuals involved in animal handling, exposure, necropsy, and lesion scoring were blinded to the exposure conditions.

The skin of the left thorax and ventral neck was shaved with an electric clipper. A cannula (PE-10, Clay Adams, Franklin Lakes, NJ) was placed into the right external jugular vein through a ventral midline incision in the neck for injection of supplemental anesthetic and paralytic agent, and a tracheotomy was also performed. Following the surgical preparation, the anesthetized rats rested for approximately 15 min during which time preparation for ultrasound exposure was completed. A depilatory agent (Nair,® Carter-Wallace, Inc., New York, NY) was used on the skin of the left thorax to maximize sound transmission. Three black dots were placed on the skin over the intercostal spaces between the fourth and fifth ribs, sixth and seventh ribs, and eighth and ninth ribs to guide the positioning of the ultrasonic beam. The center-to-center rib spacing of rats this size is about 5 mm,[37] and thus the distance between each black dot was 1 cm. The beamwidth at the pleural surface was 610 μm, thus preventing the overlapping of exposures. Respiration was suspended by paralyzing the animals with an intravenous injection of gallamine triethiodide (5–10 mg/kg, Sigma, St. Louis). Each rat was also placed on a ventilator (Model CTE-930 ventilator, CWE, Inc., Ardmore, PA) at a respiratory rate of 60 breaths/min and a tidal volume of approximately 4 mL with 100% oxygen. Total experimental time following paralysis was not longer than the effective dose of gallamine nor longer than the effective dose time of the anesthetic. Body temperature was maintained at 36.5–37.5 °C via a heating pad and radiant heat lamp.

Anesthetized rats were placed in right lateral recumbancy and a stand-off tank (degassed water; 30 °C) positioned in contact with the skin (Fig. 1). The circular transducer holder was visually centered above each black dot. The transducer was placed in the holder that was in the stand-off

tank. The low-power (*in vivo* peak rarefactional pressure of 0.4 MPa, *in vivo* peak compressional pressure of 0.5 MPa, pulse repetition frequency of 10 Hz, Mechanical Index of 0.13) pulse-echo capability of the exposure system (RAM5000, Ritec, Inc., Warwick, RI) displayed on an oscilloscope was used to adjust the axial center of the focal region to within 1 mm of the lung surface. Thus the ultrasonic beam was approximately perpendicular to the skin at the position of the black dot with the beam's focal region at the lateral surface of the lung, and approximately normal to the lung's pleural surface. This alignment procedure was repeated for each exposure.

For each rat, the same ultrasound exposure conditions were used at each exposure site. The volume of pulmonary inflation was varied for each rat. Three lung-inflation conditions were utilized in each rat. The second ultrasound exposure of the three was with the lung inflated. The first and third exposures were randomized either with the lung deflated or half-deflated. In a previous rat study[38] five adjacent lesions of equal size were created using the same superthreshold exposure conditions. Also, the same 3.1-MHz transducer used herein was used for this previous study. The exposure sites were located in the five adjacent intercostal spaces between the fourth and ninth ribs. This suggested that sensitivity across the lung surface does not change. Therefore, randomizing the location of the three exposure sites was not considered necessary.

Lung inflation was generated by attaching a 10-cc syringe to the tracheotomy tube after which air was pushed into the lungs. Two volumes of lung inflation (6 mL for the larger volume and 3 mL for the smaller volume) were generated to test for ultrasound-induced damage. Tidal volume for ventilation of rats was estimated from the allometric equation $\text{Tidal Volume}=7.69\text{M}^{1.04}$ (Ref. 39) where M equals the mass of the animal in grams and tidal volume is expressed in mL. Tidal volume for each rat was estimated prior to the experiment and the volume of inspired air was adjusted on the ventilator. In all cases, the maximal inspired volume (2 $\times$tidal volume) was well under vital capacity of the lungs[39] so as to prevent overinflation lung damage. The larger lung inflation volume was approximately 20% greater than tidal volume (TV) and the smaller lung inflation volume was 60% less than tidal volume (HTV). The lung inflation state was held constant for the duration of the ultrasound exposure (10 s). The smallest lung volume was achieved by detaching the ventilator from the tracheotomy tube and allowing the lungs to assume a volume at functional residual capacity (FRC). During all states of lung inflation a distinct apnea was associated with the ultrasound exposure period as determined by lack of chest wall movement.

Following the ultrasound exposure procedures, rats were euthanized under anesthesia by cervical dislocation. The thorax was opened and the thickness of each left thoracic wall (skin, rib cage, and parietal pleura) was measured at the point of exposure over the middle black dot using a digital micrometer (accuracy: 10 μm). These chest wall measurements were used for later calculation of the *in situ* ultrasonic pressures at the visceral pleural surface. Lungs were removed, rinsed in 0.9% sodium chloride, examined grossly for the presence or absence of lesion(s), and then photographed digitally. Each lung was placed in a sterile 50-mL clear polypropylene centrifuge tube and was fixed by immersion in 10% neural-buffered formalin for a minimum of 24 h. After total fixation, the elliptical dimensions of lung lesions at the visceral pleural surface were measured with a digital micrometer (accuracy: 10 μm), where "*a*" was the length of the semi-major axis and "*b*" was the length of the semi-minor axis. The lesions were then bisected and the depth "*d*" of the lesion within the lung was measured. In animals where the depth of the lesion was not visually discernible, the depth was determined from measurements made on histologic sections with a slide micrometer. The surface area (πab) and volume ($\pi abd/3$) of the lesion were calculated for each animal. Each half of the bisected lesion was embedded in paraffin, sectioned at 5 μm, stained with hematoxylin and eosin, and evaluated microscopically.

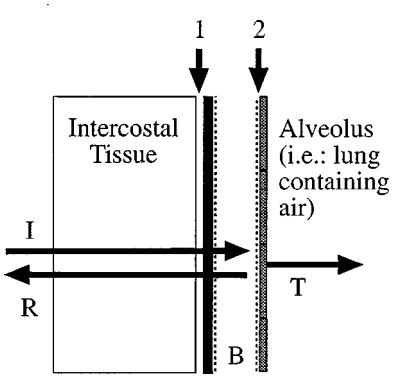

FIG. 2. Schematic diagram of the interface zone between intercostal tissue and lung (not to scale). The innermost layer of the intercostal tissue within the thoracic cavity is covered with parietal pleural. The lung is covered by visceral pleura (thick black line) and the two pleural layers glide over each other during the respiratory cycle. The space (thoracic cavity—arrow 1) between the two pleura layers is under negative pressure. The visceral pleura contains blood-filled capillaries (B) lined by a single layer of endothelial cells (open rectangles). The alveolus (air-filled) is separated from blood in the capillary by a single trilaminar membrane called the air–blood barrier (arrow 2). This barrier is formed by type 1 alveolar epithelial cells (filled rectangles), basement membrane, and capillary endothelial cells. It can measure as thin as 100 nm in some areas. Acoustic boundary conditions may exist and play a role in ultrasound-induced lung hemorrhage at the air-blood barrier (arrow 2). I=incident sound; R=reflected sound; T=transmitted sound.

III. APPLICATION ACOUSTIC THEORY

The acoustic impedance of the intercostal tissue and lung was evaluated to understand the acoustic propagation at and across the boundary. Figure 2 defines the boundary. In a previous study,[17] hydrostatic-pressure changes along could not explain the enhanced effects on lung hemorrhage. It was thus speculated that if the mouse's breathing pattern were altered as a function of hydrostatic pressure, and this alteration affected the volume of air inspired and expired, then an increase in the power transmitted into lung might occur. Therefore, for the study reported herein, the rat's inspiration was controlled, and thus the amount of air in the lung was the main experimental variable.

A planar boundary was assumed between intercostal tissue and lung with the incident ultrasonic field in the inter-

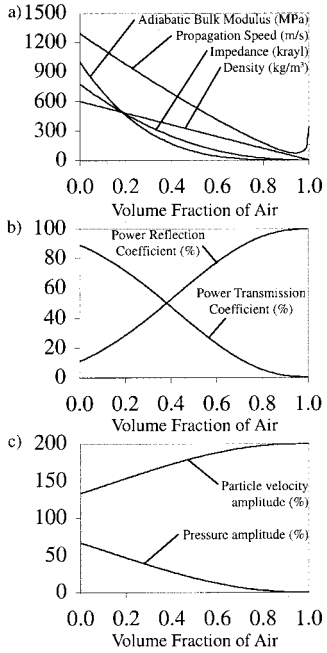

FIG. 3. (a) Adiabatic bulk modulus, propagation speed, characteristic acoustic impedance, and density of lung as a function of volume fraction of air in the lung. These curves were calculated from Eqs. (2), (3), (4), and (1), respectively. (b) Sound power reflection coefficient and sound power transmission coefficient as a function of volume fraction of air in the lung. These curves were calculated from Eqs. (5) and (6), respectively. (c) Particle velocity amplitude and acoustic pressure amplitude near the lung surface as a function of volume fraction of air in the lung. These curves were calculated from Eqs. (8) and (7), respectively.

costal tissue and the ultrasonic beam axis normal to the boundary. Lung was modeled as two components consisting of air and parenchyma where the lung's density is

$$\rho_{\text{lung}} = x_{\text{air}}\rho_{\text{air}} + x_{\text{parenchyma}}\rho_{\text{parenchyma}}, \tag{1}$$

the lung's adiabatic bulk modulus is

$$B_{\text{lung}} = x_{\text{air}}B_{\text{air}} + x_{\text{parenchyma}}^{3.5}B_{\text{parenchyma}}, \tag{2}$$

and the volume fractions of air and parenchyma sum to unity, that is, $x_{\text{air}} + x_{\text{parenchyma}} = 1$. This model was selected because it fit the experimental measurements of reflection coefficient versus lung inflation in the fixed lungs of dogs at 2.4 MHz,[40] and the experimental measurements of propagation speed at one lung inflation in fresh lungs of dogs at 2.25 MHz.[41] The fit to these published measurements yielded $\rho_{\text{air}} = 1.21$ kg/m^3, $\rho_{\text{parenchyma}} = 600$ kg/m^3, $B_{\text{air}} = 142$ kPa, and $B_{\text{parenchyma}} = 1$ GPa for $x_{\text{air}} = 0.31$, and, in turn, yielded $\rho_{\text{lung}} = 414$ kg/m^3 and $B_{\text{lung}} = 273$ MPa. Propagation speed is determined from

$$c_{\text{lung}} = \sqrt{B_{\text{lung}}\rho_{\text{lung}}}, \tag{3}$$

and acoustic impedance is determined from

$$z_{\text{lung}} = \sqrt{\rho_{\text{lung}}B_{\text{lung}}}. \tag{4}$$

These fit values agreed well with published results. The fit reflection coefficient value relative to 1.5 Mrayl was -7.7 dB; the published values were between -2 and -4 dB.[40] The fit and published[41] lung propagation speed values were 812 m/s.

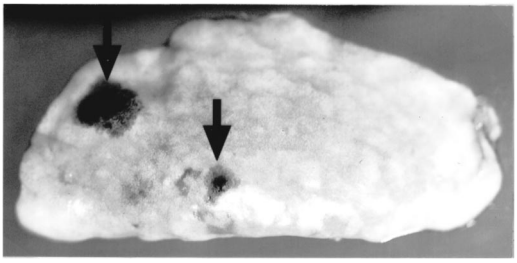

FIG. 4. Rat lung (R1694). Lung was exposed at superthreshold condition (*in situ* peak rarefactional pressure of 16 MPa) to ensure the formation of lesions. Arrows represent foci of lung hemorrhage caused by ultrasound exposure. The hemorrhage (depth=2.60 mm; area=2.54 mm^2; volume=2.20 mm^3) labeled by the right arrow (cranial most exposure) occurred when the lung was exposed under the "half-deflated" state. The hemorrhage (depth =2.92 mm; area=12.96 mm^2; volume=12.61 mm^3) labeled by the left arrow (caudal most exposure) occurred when the lung was exposed under the "deflated" state. The region of lung between the two areas of hemorrhage, which had no lesion, was exposed to ultrasound when the lung was under the "inflated" state.

The density and adiabatic bulk modulus of lung [from Eqs. (1) and (2)], along with their propagation speed and characteristic acoustic impedance [from Eqs. (3) and (4)] are graphed [Fig. 3(a)] as a function of the amount of air in lung. The four constant quantities used in Eqs. (1) and (2) were $\rho_{\text{air}} = 1.21$ kg/m^3, $\rho_{\text{parenchyma}} = 600$ kg/m^3, $B_{\text{air}} = 142$ kPa, and $B_{\text{parenchyma}} = 1$ GPa, and the one variable was $0 \leqslant x_{\text{air}} \leqslant 1$ where $x_{\text{parenchyma}} = 1 - x_{\text{air}}$.

The power reflection coefficient (R_π) and power transmission coefficient (T_π) were determined to assess the power transfer at the intercostal tissue-lung boundary. At normal incidence to the planar boundary, these quantities (which are the same as the intensity reflection and transmission coefficients at normal incidence) are given by

$$R_\pi = \left(\frac{z_{\text{lung}} - z_{\text{intercostal tissue}}}{z_{\text{lung}} + z_{\text{intercostal tissue}}}\right)^2, \tag{5}$$

$$T_\pi = \frac{4z_{\text{lung}}z_{\text{intercostal tissue}}}{(z_{\text{lung}} + z_{\text{intercostal tissue}})^2}, \tag{6}$$

where $z_{\text{intercostal tissue}}$ is 1.54 Mrayl. The power reflection and transmission coefficients are graphically shown as a function of the amount of air in lung in Fig. 3(b).

It had been previously hypothesized that because the lung boundary acts as an acoustic pressure-release surface, and if constructive interference occurred near to the lung surface, then there would be a significant increase in pressure *in situ*.[9,42] Though it is particle velocity that is a maximum right at the lung surface at a pressure-release surface, the pressure is significantly increased only one quarter of a wavelength into the intercostal tissue from that surface, so their idea has merit and is evaluated. The acoustic pressure (p_0) and particle velocity (u_0) amplitudes in the intercostal tissue and near the lung surface where constructive interference can be presumed are given by

$$p_0 = (1 + R)p_{in\ situ}, \tag{7}$$

$$u_0 = (1 - R)\frac{p_{in\ situ}}{z_{\text{intercostal tissue}}}, \tag{8}$$

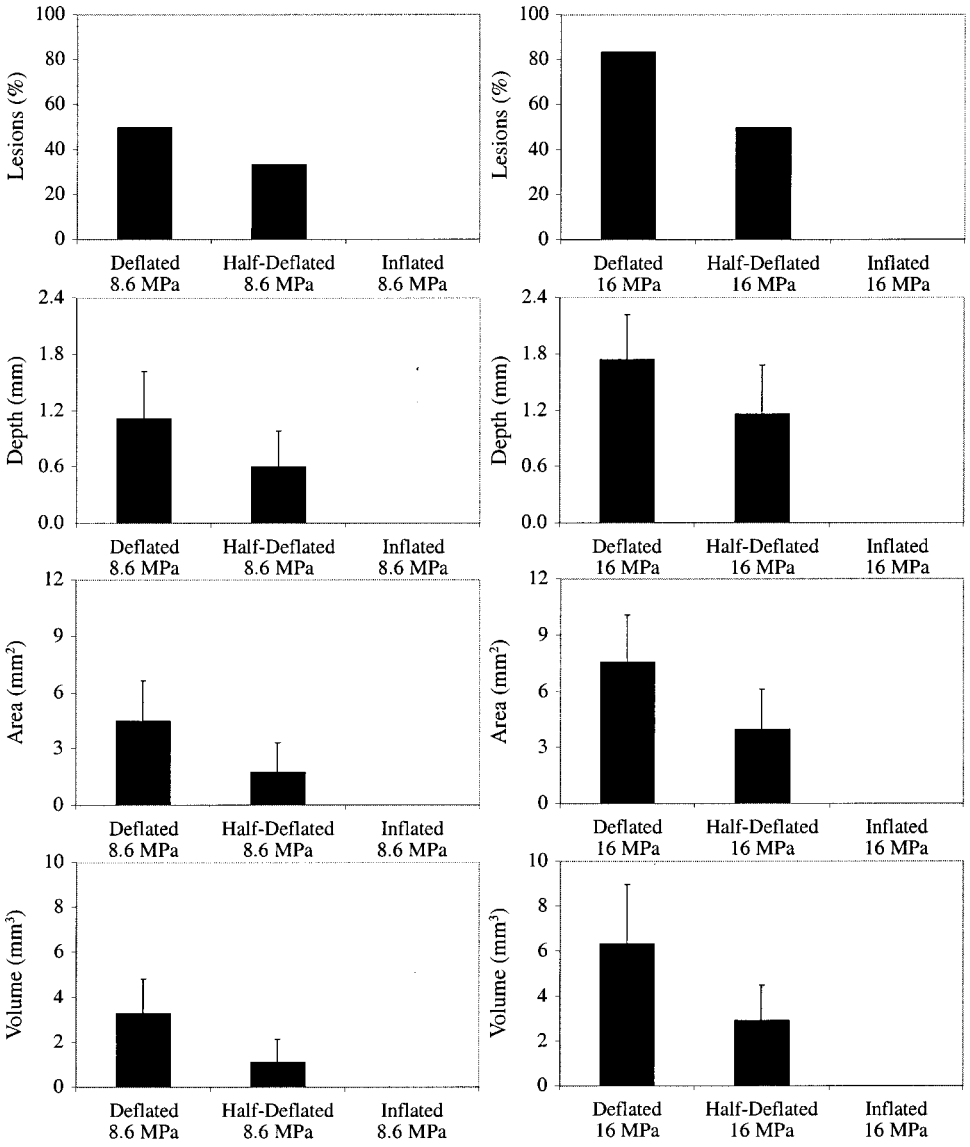

FIG. 5. Lesion occurrence, depth, surface area, and volume as a function of the three states of lung inflation (deflated, half-deflated, inflated). The four left-hand panels are for an *in situ* peak rarefactional pressure of 8.6 MPa. The four right-hand panels are for an *in situ* peak rarefactional pressure of 16 MPa.

where $p_{in\ situ}$ is the *in situ* (at the pleural surface) acoustic pressure amplitude, and R is the sound pressure reflection coefficient at normal incidence given by

$$R = \frac{z_{\text{lung}} - z_{\text{intercostal tissue}}}{z_{\text{lung}} + z_{\text{intercostal tissue}}}. \tag{9}$$

The acoustic pressure and particle velocity amplitudes relative to values for the incident wave [from Eqs. (7) and (8)] are shown graphically as a function of the amount of air in lung in Fig. 3(c).

IV. RESULTS

A. Gross and histological observations

A red-to-dark elliptical area of hemorrhage that formed along the pathway of the ultrasound beam was visible on the visceral pleural surface (Fig. 4). The hemorrhage assumed a conical shape whose base opposed the visceral pleural surface and whose apex extended into subjacent lung parenchyma to varied depths within the lung. Microscopically, the lesion was alveolar hemorrhage; alveolar septa did not appear injured. The principle tissue affected was the microvasculature.

B. Lesion occurrence and size

Lesion occurrence is related to the degree of inflation wherein there are a greater number of lesions for FRC volume (deflated lung state), fewer lesions for HTV (half-deflated lung state), and no lesions for the TV lung volume (inflated lung state). Lesion occurrence was also related to $p_{r(in\ situ}$ (Fig. 5) wherein there were a greater number of lesions at the higher $p_{r(in\ situ)}$ value compared to the lower $p_{r(in\ situ)}$ value.

Lesion size (depth, surface area, and volume) had a similar pattern as that for lesion occurrence (Fig. 5). Lesion size was larger for the higher $p_{r(in\ situ)}$ value (16 MPa) compared to the lower $p_{r(in\ situ)}$ value (8.6 MPa). Lesion size was also related to the degree of inflation wherein the lesions were largest for the deflated lung state [mean (SEM) depth: 1.11(0.50) and 1.74(0.48) mm for 8.6 and 16 MPa, respectively; mean area (SEM): 4.48(2.15) and 7.59(2.51)

mm^2 for 8.6 and 16 MPa, respectively], intermediate in size for the half-deflated lung state [mean (SEM) depth: 0.60(0.38) and 1.16(0.52) mm for 8.6 and 16 MPa, respectively; mean area(SEM): 1.72(1.60) and 3.97(2.15) mm^2 for 8.6 and 16 MPa, respectively], and were not initiated under the inflated lung state. A single-factor ANOVA yielded no statistically significant differences for lesion size at the lower $p_{r(in\ situ)}$ value (depth: $p=0.13$; area: $p=0.15$; volume: $p=0.12$). However, a single-factor ANOVA yielded marginally statistically significant differences for lesion size at the higher $p_{r(in\ situ)}$ value (depth: $p=0.03$; area: $p=0.04$; volume: $p=0.07$).

V. DISCUSSION

The magnitude of the acoustic pressure was selected for this study with the intent that it would be large enough to ensure that an ultrasound-induced lesion was produced every time. The *in situ* peak rarefactional pressures of 8.6 and 16 MPa (*in situ* peak compressional pressure of 18 and 40 MPa, respectively) were based on our previous findings.[18–20] These values bracket the peak *in situ* rarefactional pressure of 11 MPa at which the percentage of rats with lesions was 80% at an ultrasonic frequency of 2.8 MHz and 10-s exposure duration in normal breathing animals. We recognized that *in situ* peak rarefactional pressures of 8.6 and 16 MPa were considerably greater than those allowed under current regulations.[43] At these *in situ* peak rarefactional pressures, the equivalent Mechanical Indices were 3.1 and 5.6, whereas the regulatory limit is 1.9 for diagnostic ultrasound equipment that falls under FDA control. Our purpose was to evaluate the effect of lung inflation at superthreshold exposure conditions.

At the lower $p_{r(in\ situ)}$ value (8.6 MPa), the two measured lesion quantities, depth, and area, were not significantly different whereas, at the higher $p_{r(in\ situ)}$ value (16 MPa), these two quantities were significantly different. This demonstrated that as $p_{r(in\ situ)}$ increases, there was increased lesion size separation.

The 3.1-MHz results reported herein are directly compared to one of our previous studies in which we conducted an exposure-effect study at two frequencies (2.8 and 5.8 MHz) with normal breathing adult ICR mice and Sprague-Dawley rats (Fig. 6).[18] The 2.8- and 5.6-MHz exposure conditions for the previous study were similar to the 3.1-MHz exposure conditions used herein (1-kHz PRF, 10-s exposure duration). In that previous study, there were no differences in occurrence (percentage) of lesions with either species or ultrasound frequency. Also, there was no dependence on frequency for either lesion depth or area, although there was a small dependence on species for lesion area. Lesion occurrences for the FRC state (deflated lung state) were about the same as those for the previous study. Lesion occurrences for the HTV state (half-deflated lung state) were less than those for the previous study. Lesion size (depth, surface area, and volume) for the deflated and half-deflated lung states appeared to bracket the comparable results for the normal breathing mice and rats. These observations show that lung lesions are not caused when the lungs are inflated at just over

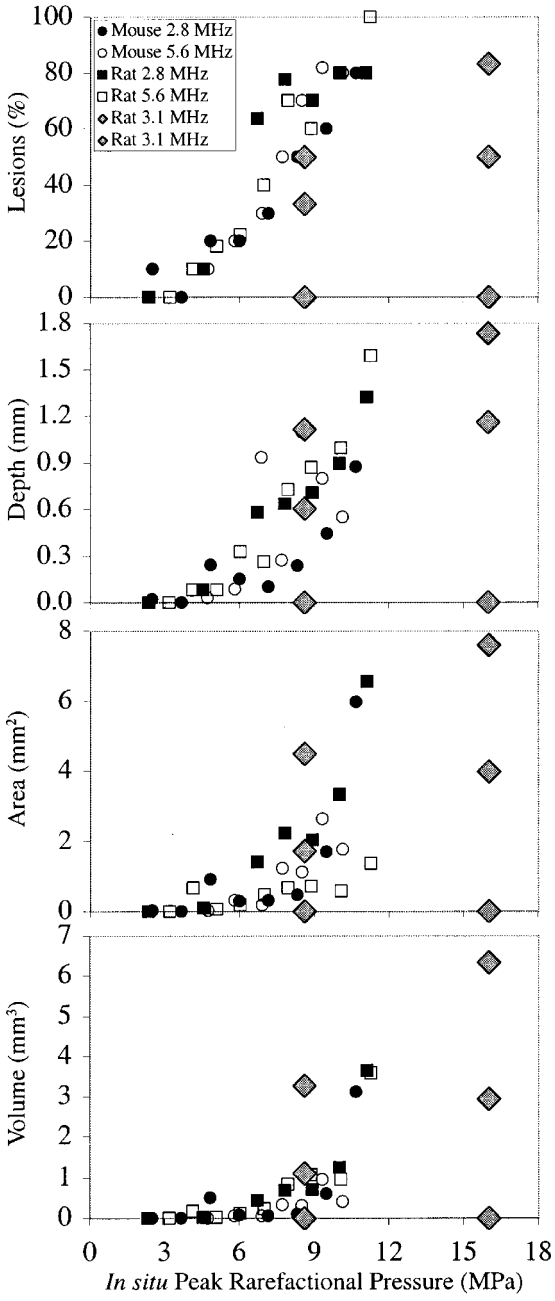

FIG. 6. Lesion occurrence, depth, surface area, and volume as a function of the *in situ* peak rarefactional pressure that compare the inflation-dependent data reported herein (large diamonds) to the previously published normal-breathing mice and rates data (Ref. 18).

tidal volume, but occur when the lung is less inflated. In fact, comparisons of the results reported herein to the normal breathing animal results suggest that the lesions occur and grow in normal breathing animals in a similar manner to lung inflation between FRC and HTC lung volumes.

Further, the extent to which lung lesions occur is inversely related to the acoustic impedance difference between intercostal tissue and lung. When the lung's acoustic impedance is more closely matched to the intercostal tissue, more lesions are produced and the sound power transmission coefficient is larger. And, a greater impedance difference produces fewer lesions and has a smaller sound power transmission coefficient. This finding suggests that the lesion cause

may be due to some kind of an energy-based mechanism within and near the lung's surface since the extent to which the lesions occur is directly related to the sound power transmission coefficient. Also, for all three lung inflation states, air is present in the lung, and yet, at tidal volume no lesions are produced.

The findings reported herein address the suggestion put forth earlier[6,42] that because the lung boundary acts as an acoustic pressure-release surface, a significant increase in particle velocity *in situ* near the lung surface might produce the lung hemorrhage. This suggestion is not plausible for the following reasons. A pressure-release surface would be approached when the lung is inflated (volume fraction of air in lung approaches unity). Under a more inflated lung state, where the lung's volume fraction of air is close to unity and the particle velocity in tissues adjacent the lung is greatest, no lung hemorrhage resulted. The lung hemorrhage increased as the lung's volume fraction of air decreased and was the greatest at the lowest volume fraction of air.

Finally, the relative geometry between the beam and the lung surface is considered for the three inflation states. The transducer alignment occurs while the ventilator is breathing for the animal. The distance between the transducer and the lung surface does not vary by more than 1–2 mm because the water filled stand-off tank is placed gently on the rat's lateral aspect, thus limiting chest expansion in that direction. The −6-dB depth of focus is 5.9 mm so the lung surface remains within the focal region for all three inflation states. Also, the orientation of the chest wall surface in contact with the water filled stand-off tank does not visually change as a function of breathing. Because the chest wall surface and the lung surface track each other, the orientation between the beam axis and the pleural surface does not change. Therefore, the observations and findings reported herein are not believed to be a function of lung surface orientation or position relative to the ultrasonic field.

ACKNOWLEDGMENTS

We thank our valued colleagues Joe Beatty, Ed Plowey, and Bill Zierfuss for technical contributions. This work was supported by NIH Grant No. HL58218 awarded to WDO and JFZ.

[1] S. Z. Child, C. L. Hartman, L. A. Schery, and E. L. Carstensen, "Lung damage from exposure to pulsed ultrasound," Ultrasound Med. Biol. **16**, 817–825 (1990).
[2] C. L. Hartman, S. Z. Child, R. Mayer, E. Schenk, and E. L. Cartensen, "Lung damage from exposure to the fields of an electron hydraulic lithotropter," Ultrasound Med. Biol. **16**, 675–683 (1990).
[3] C. H. Raeman, S. Z. Child, and E. L. Carstensen, "Timing of exposures in ultrasonic hemorrhage of murine lung," Ultrasound Med. Biol. **19**, 507–512 (1993).
[4] D. P. Penney, E. A. Schenk, K. Maltby, C. Hartman-Raeman, S. Z. Child, and E. L. Carstensen, "Morphologic effects of pulsed ultrasound in the lung," Ultrasound Med. Biol. **19**, 127–135 (1993).
[5] L. A. Frizzell, E. Chen, and C. Lee, "Effects of pulsed ultrasound on the mouse neonate: Hind limb paralysis and lung hemorrhage," Ultrasound Med. Biol. **20**, 53–63 (1994).
[6] A. F. Tarantal and D. R. Canfield, "Ultrasound-induced lung hemorrhage in the monkey," Ultrasound Med. Biol. **20**, 65–72 (1994).
[7] J. F. Zachary and W. D. O'Brien, Jr., "Lung hemorrhage induced by continuous and pulse wave ultrasound in mice, rabbits, and pigs," Vet. Pathol. **32**, 43–54 (1995).
[8] C. H. Harrison, H. A. Eddy, J.-P. Wang, and F. Z. Liberman, "Microscopic lung alterations and reduction of respiration rate in insonated anesthetized swing," Ultrasound Med. Biol. **21**, 981–983 (1995).
[9] C. K. Holland, C. X. Deng, R. E. Apfel, J. L. Alderman, L. A. Fernandez, and K. J. Taylor, "Direct evidence of cavitation in vivo from diagnostic ultrasound," Ultrasound Med. Biol. **22**, 917–925 (1996).
[10] R. Baggs, D. P. Penney, C. Cox, S. Z. Child, C. H. Raeman, D. Dalecki, and E. L. Carstensen, "Thresholds for ultrasonically induced lung hemorrhage in neonatal swine," Ultrasound Med. Biol. **22**, 119–128 (1996).
[11] C. H. Raeman, S. Z. Child, D. Dalecki, C. Cox, and E. L. Carstensen, "Exposure-time dependence of the threshold for ultrasonically induced murine lung hemorrhage," Ultrasound Med. Biol. **22**, 139–141 (1996).
[12] W. D. O'Brien, Jr. and J. F. Zachary, "Lung damage assessment from exposure to pulsed-wave ultrasound in rabbit, mouse, and pig," IEEE Trans. Ultrason. Ferroelectr. Freq. Control **44**, 473–485 (1997).
[13] D. Dalecki, S. Z. Child, C. H. Raeman, C. Cox, and E. L. Carstensen, "Ultrasonically induced lung hemorrhage in young swine," Ultrasound Med. Biol. **23**, 777–781 (1997).
[14] D. Dalecki, S. Z. Child, C. H. Raeman, C. Cox, D. P. Penney, and E. L. Carstensen, "Age dependence of ultrasonically-induced lung hemorrhage in mice," Ultrasound Med. Biol. **23**, 767–776 (1997).
[15] WFUMB Symposium on Safety of Ultrasound in Medicine: Issues and Recommendations Regarding Non-Thermal Mechanisms for Biological Effects of Ultrasound, Ultrasound Med. Biol. **24**, Supplement 1, S1–S55 (1998).
[16] *Mechanical Bioeffects from Diagnostic Ultrasound: AIUM Consensus Statements* (American Institute of Ultrasound in Medicine, Laurel, MD, 2000). Also, J. Ultrasound Med. **19**, 67–168 (2000).
[17] W. D. O'Brien, Jr., L. A. Frizzell, R. M. Weigel, and J. F. Zachary, "Ultrasound-induced lung hemorrhage is not caused by inertial cavitation," J. Acoust. Soc. Am. **108**, 1290–1297 (2000).
[18] J. F. Zachary, J. M. Sempsrott, L. A. Frizzell, D. G. Simpson, and W. D. O'Brien, Jr., "Superthreshold behavior and threshold estimation of ultrasound-induced lung hemorrhage in adult mice and rats," IEEE Trans. Ultrason. Ferroelectr. Freq. Control **48**, 581–592 (2001).
[19] W. D. O'Brien, Jr., L. A. Frizzell, D. J. Schaeffer, and J. F. Zachary, "Superthreshold behavior of ultrasound-induced lung hemorrhage in adult mice and rats: role of pulse repetition frequency and exposure duration," Ultrasound Med. Biol. **27**, 267–277 (2001).
[20] J. F. Zachary, K. S. Norrell , J. P. Blue, R. J. Miller, and W. D. O'Brien, Jr., "Temporal and spatial evaluation of lesion resolution following exposure of rat lung to pulsed ultrasound," Ultrasound Med. Biol. **27**, 829–839 (2001).
[21] W. D. O'Brien, Jr., D. G. Simpson, L. A. Frizzell, and J. F. Zachary, "Superthreshold behavior and threshold estimation of ultrasound-induced lung hemorrhage in adult rates: Role of beamwidth," IEEE Trans. Ultrason. Ferroelectr. Freq. Control **48**, 1695–1705 (2001).
[22] M. L. Crosfill and J. G. Widdicombe, "Physical characteristics of the chest and lungs and the work of breathing in different mammalian species," J. Physiol. (London) **158**, 1–14 (1961).
[23] S. M. Tenney and J. E. Remmers, "Comparative quantitative morphology of the mammalian lung: Diffusing area," Nature (London) **197**, 54–56 (1963).
[24] E. R. Weibel, "Dimensions of the tracheobronchial tree and alveoli," in *Biological Handbooks: Respiration and Circulation*, edited by P. L. Altman and D. S. Dittmer (Federation of American Societies for Experimental Biology, Bethesda, MD, 1971), pp. 930–939.
[25] H. G. Flynn and C. C. Church, "Transient pulsations of small gas bubbles in water," J. Acoust. Soc. Am. **84**, 985–998 (1988).
[26] M. R. Bailey, D. Dalecki, S. Z. Child, C. H. Raeman, D. P. Penney, D. T. Blackstock, and E. L. Carstensen, "Bioeffects of positive and negative acoustic pressures *in vivo*," J. Acoust. Soc. Am. **100**, 3941–3946 (1996).
[27] E. L. Carstensen, D. Dalecki, S. M. Gracewski, and T. Christopher, "Nonlinear propagation of the output indices," J. Ultrasound Med. **18**, 69–80 (1999).
[28] C. K. Holland, R. A. Roy, P. W. Biddinger, C. J. Disimile, and C. Cawood, "Cavitation mediated rat lung bioeffects from diagnostic ultrasound," J. Acoust. Soc. Am. **109**, 2433(A) (2000).
[29] R. E. Apfel, "Comments on 'Ultrasound-induced lung hemorrhage is not caused by inertial cavitation' [J. Acoust. Soc. Am. **108**, 1290–1297 (2000)]," J. Acoust. Soc. Am. **110**, 1737 (2001).
[30] L. A. Frizzell, J. M. Kramer, J. F. Zachary, and W. D. O'Brien, Jr.,

''Response to ''Comments on 'Ultrasonic lung hemorrhage is not caused by inertial cavitation' '' [J. Acoust. Soc. Am. **110**, 1737 (2001)],'' J. Acoust. Soc. Am. **110**, 1738–1739 (2001).
[31] R. E. Apfel, ''Reply to Frizzell *et al.*'s Comment to our comment,'' J. Acoust. Soc. Am. **110**, 1740–1741 (2001).
[32] L. A. Frizzell, J. M. Kramer, J. F. Zachary, and W. D. O'Brien, Jr., ''Comment on Apfel's second comment,'' J. Acoust. Soc. Am. **110**, 1742 (2001).
[33] K. Raum and W. D. O'Brien, Jr., ''Pulse-echo field distribution measurement technique of high-frequency ultrasound sources,'' IEEE Trans. Ultrason. Ferroelectr. Freq. Control **44**, 810–815 (1997).
[34] *AIUM/NEMA, Acoustic Output Measurement Standard for Diagnostic Ultrasound Equipment*, Laurel, MD, American Institute of Ultrasound in Medicine, and Rosslyn, VA, National Electrical Manufacturers Association, 1998.
[35] *Standard for Real-Time Display of Thermal and Mechanical Acoustic Output Indices on Diagnostic Ultrasound Equipment, Rev. 1*, Laurel, MD, American Institute of Ultrasound in Medicine, and Rosslyn, VA, National Electrical Manufacturers Association, 1998.
[36] J. M. Sempsrott and W. D. O'Brien, Jr., ''Experimental verification of acoustic saturation,'' Proceedings of the 1999 IEEE Ultrasonic Symposium, pp. 1287–1290 (1999).
[37] G. A. Teotico, R. J. Miller, L. A. Frizzell, J. F. Zachary, and W. D. O'Brien, Jr., ''Attenuation coefficient estimates of mouse and rate chest wall,'' IEEE Trans. Ultrason. Ferroelectr. Freq. Control **48**, 593–601 (2001).
[38] J. M. Kramer, T. G. Waldrop, L. A. Frizzell, J. F. Zachary, and W. D. O'Brien, Jr., ''Cardiopulmonary function in rats with lung hemorrhage induced by pulsed ultrasound exposure,'' J. Ultrasound Med. **20**, 1197–1206 (2001).
[39] W. R. Stahl, ''Scaling of respiratory variables in mammals,'' J. Appl. Physiol. **22**, 453–460 (1967).
[40] T. J. Bauld and H. P. Schwan, ''Attenuation and reflection of ultrasound in canine lung tissue,'' J. Acoust. Soc. Am. **56**, 1630–1637 (1974).
[41] F. Dunn, ''Attenuation and speed of ultrasound in lung,'' J. Acoust. Soc. Am. **56**, 1638–1639 (1974).
[42] C. K. Holland, K. Sandstrom, X. Zheng, J. Rodriguey, and R. A. Roy, ''The acoustic field if a pulsed Doppler diagnostic ultrasound system near a pressure-release surface,'' J. Acoust. Soc. Am. **95**, 2855(A) (1994).
[43] *Information for Manufacturers Seeking Marketing Clearance of Diagnostic Ultrasound Systems and Transducers*, Rockville, MD, Center for Devices and Radiological Health, US Food and Drug Administration, September 30, 1997.